Journal of Applied Fluid Mechanics, Vol. 18, No. 6, pp. 1502-1511, 2025.
Available online at www.jafmonline.net, ISSN 1735-3572, EISSN 1735-3645.
https://doi.org/10.47176/jafm.18.6.3165

Effect of Gate Opening Height on the Hydraulic Jump Characteristics in an Open Channel

P. D. Jiwane[1†], A. D. Vasudeo[1] and A. K. Singh[2]

[1] *Department of Civil Engineering, Visvesvaraya National Institute of Technology, Nagpur, Maharashtra, 440010, India*
[2] *Department of Mechanical Engineering, Visvesvaraya National Institute of Technology, Nagpur, Maharashtra, 440010, India*

†*Corresponding Author Email: dt20civ002@students.vnit.ac.in*

ABSTRACT

Hydraulic jump is often used to dissipate energy of flow in open channels. Despite extensive study on hydraulic jump, effects of tail gate operation on hydraulic jump remains underexplored in the standard literature. This research investigates the effects of sluice gate opening (SGO) and tail gate opening (TGO) on hydraulic jump characteristics using experiments, theoretical analysis, and numerical simulations. The study is carried out for Froude Number range of 1.58 - 4.48, SGO range of 0.011 – 0.020 m and TGO range of 0.023 – 0.030 m. The results show that increasing sluice gate opening (SGO) primarily affects the hydraulic jump location, moving it closer to the sluice gate and reducing upstream depth (y_1), while downstream depth (y_2) remains almost same. On the other hand, there is substantial increase in downstream depth (y_2) and the location of hydraulic jump shifts towards sluice gate with decreasing tail gate opening (TGO). Locations of the hydraulic jump are estimated using theoretical equation, experiments and numerical simulations. In addition, energy dissipation analysis reveals that TGO is more effective than SGO in dissipating energy through hydraulic jumps.

Article History

Received October 7, 2024
Revised January 21, 2025
Accepted January 23, 2025
Available online March 30, 2025

Keywords:

Hydraulic jump
Tail gate opening
Jump location
Energy dissipation
Flow-3D

1. INTRODUCTION

Hydraulic jump is characterized by abrupt transition from supercritical flow to subcritical flow in a channel, resulting in an immediate rise in water depth (Subramanya, 2019). Hydraulic jump is often associated with formation of surface rollers, intense mixing, air entrainment, energy dissipation etc. (Gharangik & Chaudhry, 1991). When designing the hydraulic structures, estimating the flow depth, location of the hydraulic jump and the amount of dissipated energy is crucial to prevent the damages due to supercritical flow on the structure. It has been observed that the gates are frequently utilized due to their ability to control the water levels and hydraulic jumps, measurement of flow discharge and ease of construction (Mirzaei & Tootoonchi, 2020). Chow (1959) explored water surface profiles of hydraulic jump transitioning from supercritical to subcritical region. Several experimental, theoretical, and numerical studies have been conducted to investigate the characteristics of hydraulic jump including flow depth and location of the jump (Hager & Bremen, 1989; Gharangik & Chaudhry, 1991; Singha et al., 2005; Chanson, 2009; Castro-Orgaz & Hager, 2009; Wang & Chanson, 2015; Roushangar et al., 2018; Nandi et al., 2020; Retsins & Papanicolaou, 2020; Hafnaoui & Debabeche, 2021; Mnassri & Trikki, 2022). Hager and Bremen (1989) examined the effect of wall friction, inflow Reynolds number, and aspect ratio on the sequent depths of the hydraulic jumps. Through experimental analysis, they demonstrated deviations from the Bélanger equation, especially at small inflow depths, and provides refined models to account for viscous and frictional effects on jump behavior. Gharangik and Chaudhry (1991) employed the Saint Venant equations to predict hydraulic jump across a Froude number range of 2.30 to 7.00. They validated the accuracy of the predicted flow depth and location of hydraulic jump with the experimental results. Singha et al. (2005) derived a scaling relation for the position of hydraulic jump using hydrodynamic equations. They examined the flow depth profile before and after the jump under different boundary conditions. Chanson (2009) conducted a comprehensive survey of experimental studies on hydraulic jumps, focusing on turbulent flows, undular hydraulic jumps, positive surges, and tidal bores. The study also highlighted the effects of air entrainment, turbulent mixing and scaling on hydraulic jump. Castro-Orgaz and Hager (2009) proposed a model for prediction of flow profiles of classical hydraulic jump. They highlighted the study of Froude number, non- uniform

NOMENCLATURE

d_s	sluice gate opening	Fr	Froude number
E	specific energy	n	Manning's constant
g	acceleration due to gravity	S_f	energy slope.
SGO	Sluice Gate Opening	S_0	bed slope of channel
$\overline{S_f}$	change in energy slope	V	flow velocity
TGO	Tail Gate Opening	y	flow depth at corresponding Δx
x	location of hydraulic jump	y_1	upstream flow depth of hydraulic jump
ΔE	energy loss	y_2	downstream flow depth of hydraulic jump
d_t	tail gate opening	Δx	step size theoretical location of jump

velocity profiles, and energy dissipation, using 2D models that matches well with experimental data. Wang and Chanson (2015) conducted experiments on hydraulic jumps with varying Froude numbers (3.8–8.5) and examined turbulent fluctuations near the jump toe. The results highlighted both fast and slow oscillations of the jump toe position, influenced by gate opening and inflow conditions, providing valuable insights into jump roller dynamics and energy dissipation mechanisms. Roushangar et al. (2018) effectively predicted the sequent depth ratio, length and other characteristics of the hydraulic jump under varying boundary conditions using ANFIS. Nandi et al. (2020) developed a predictive equation for hydraulic jump location based on experimental and numerical results for both horizontal and sloping beds. Furthermore, Hafnaoui and Debabeche (2021) used 2D Iber software to numerically simulate the distance and flow profile of hydraulic jumps, finding a good match between the simulation results and the experiments.

Extensive research has been carried out on the use of sluice gate for hydraulic jump and energy dissipation (Rajaratnam, 1977; Ohtsu & Yasuda, 1994; Chern & Syamsun, 2013; Gupta & Ojha, 2013; Kim et al., 2015; Gumus et al., 2016; Yildiz et al., 2020; Mirzaei & Tootoonchi, 2020; Singh & Roy, 2022). Rajaratnam (1977) investigated free flow below sluice gates, emphasizing the effect of gate opening on contraction coefficients and supercritical stream behavior and compared the theoretical studies with the experiments. Ohtsu and Yasuda (1994) examined the impact of supercritical flow on hydraulic jump. They explored the sensitivity of jump location to tailwater levels, validating predictions of velocity profiles and water surface behavior through experiments. Gupta and Ojha (2013) highlighted the effects of the vertical lift gates on the distance and depth of the hydraulic jump for different gate openings. Kim et al. (2015) studied hydraulic jump and energy dissipation with fixed and movable weirs. They reported that use of energy dissipators along the weirs is desirable for maximum energy dissipation. Gumus et al. (2016) studied submerged hydraulic jump by conducting experiments as well as numerical simulations under a sluice gate for investigating free surface flows. Singh and Roy (2022) used perforated screens for energy dissipation of the supercritical flow in the channel. They reported that perforated screens contributed more significant energy dissipation than classical hydraulic jump.

In recent times, computational fluid dynamics (CFD) software such as OpenFOAM and FLOW-3D have been utilized for simulating hydraulic jump numerically (Babaali et al., 2014; Bayón et al., 2016; Mirzaei & Tootoonchi, 2020; Paik & Kim, 2023). Babaali et al. (2014) compared two turbulence models, namely the k-ε and the RNG in FLOW-3D, with experimental data to study hydraulic jump in the convergence stilling basin. Bayón et al. (2016) also analyzed the several characteristics of hydraulic jump using the CFD softwares i.e., OpenFOAM and FLOW-3D. Mirzaei and Tootoonchi (2020) examined the effects of bump location, flow rate, and channel slope on location of hydraulic jump by varying the depth of the sluice gate as well as the location of the bump with experiments and FLOW-3D simulations. They observed the hydraulic jump moving downstream as the bump moves downstream or as discharge increases. Paik and Kim (2023) utilized large eddy simulations and VoF technique to predict the minimum pressure distribution of steady hydraulic jump at Froude number 7.3. The numerical simulations displayed a good agreement with the experiments.

Previous studies have examined the effects of sluice gate on hydraulic jump characteristics using experiments and numerical analysis. Although previous studies had used tail gate for the formation of hydraulic jump, the present literature survey reveals a lack of experimental or numerical studies regarding the role of tail gates in controlling the flow depth, location and energy dissipation of hydraulic jump in an open channel. Also, supercritical flow in the channel poses challenges such as bed damages due to high velocity, and addressing these issues requires an understanding of hydraulic jump and energy dissipation. Tail gates offer several advantages: ease of installation, simple operation, and precise control over flow conditions, making them more convenient and feasible option as compared to other devices such as weirs, sills and perforated screens. Motivated by this observation and identifying the gap that effects of tail gate on hydraulic jump is underexplored, the objective of the present study is to investigate the effects of sluice gate opening (SGO) as well as tail gate opening (TGO) on hydraulic jump, using experiments, theoretical analysis, and FLOW-3D simulations. The focus is on how tail gate can effectively control the hydraulic jump location within the channel and serve as a significant tool for energy dissipation, thereby preventing potential damage caused by supercritical flow.

2. DETAILS OF PHYSICAL MODEL

The schematic diagram of laboratory experimental set up is presented in Fig. 1 (a). The set up consisted of a

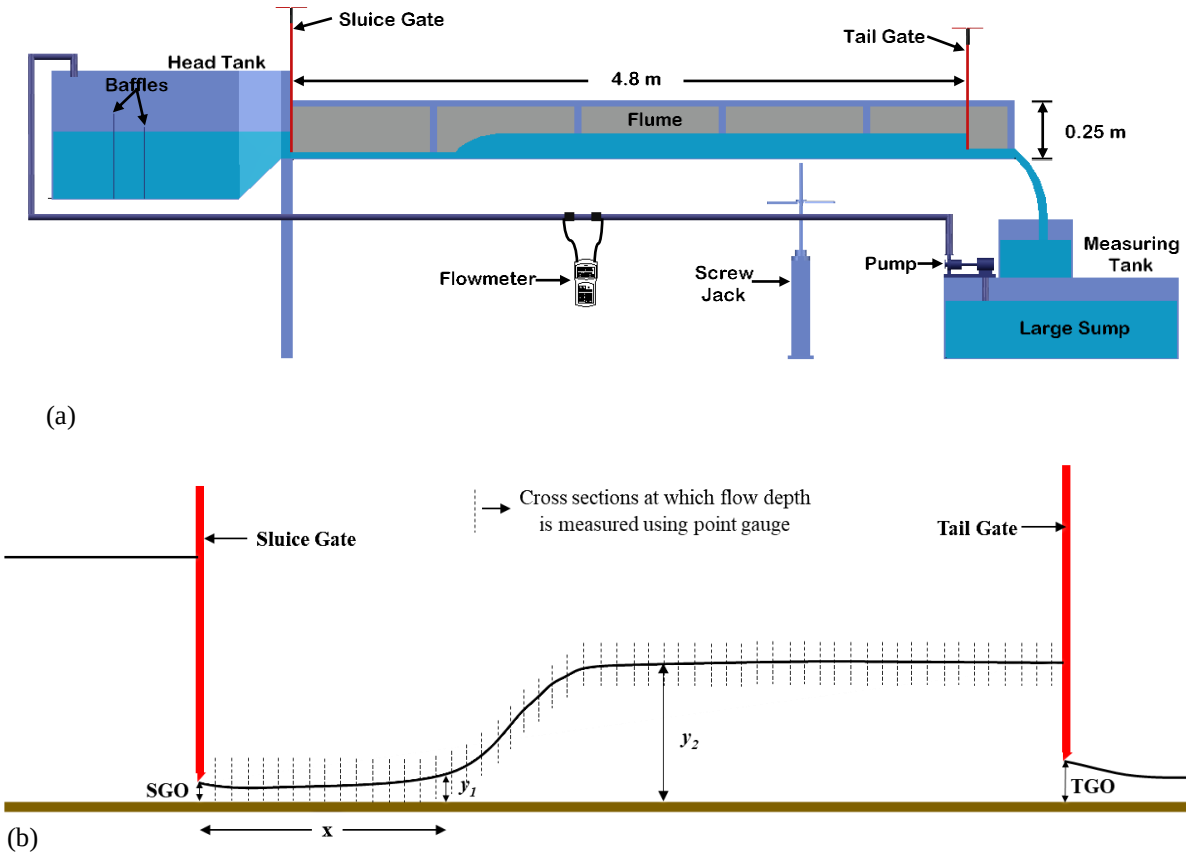

Fig. 1 (a) Schematic diagram of the Laboratory Experimental Setup, (b) Sketch of hydraulic jump including hydraulic parameters y_1, y_2, x, SGO and TGO

Table 1 Details of Experimental Setup

Parameter	Details
Bed Width	0.1 m
Height of Channel	0.25 m
Length of Channel	4.8 m
Bed Slope	Horizontal
Discharge	1.51×10^{-3} m^3/sec
SGO	0.011 – 0.020 m
TGO	0.023 – 0.030 m
Froude Number	1.58 - 4.48

rectangular perspex flume with dimensions of 0.10 m in width, 0.25 m in height, and 4.80 m in length (Table 1). Water was supplied from a large sump tank to a constant-head tank and then to the flume through a sharp-edged sluice gate. A tail gate at the downstream end of the flume was used to regulate water depth and control the hydraulic jump's position. Water from the flume discharged into the measuring tank. The flow depth profile along the flume was measured at equally spaced intervals using a point gauge with a precision of ±0.5 mm in steady flow conditions. At the same time, discharge was measured using a calibrated ultrasonic flow meter (MicroSet® company make, available at VNIT, Nagpur) and a measuring tank. Figure 1 (b) depicts the sketch of hydraulic parameters significant for this study viz. Sluice Gate Opening (SGO), Tail Gate Opening (TGO), hydraulic jump - upstream flow depth (y_1), downstream flow depth (y_2), location of jump from sluice gate (x).

The experiments were carried out to investigate the hydraulic jump and its location in the flume between sluice and tail gates by varying SGO and TGO. The hydraulic jump in a rectangular horizontal channel is depicted in Fig. 2. The flow was allowed to get steady, and then the flow surface profile of hydraulic jump along the channel was recorded with point gauge.

3. NUMERICAL SIMULATIONS

The present study utilizes FLOW-3D® HYDRO (Version 2023R1; 2023) software, which employs the Reynolds-averaged Navier–Stokes equation to solve flow problems, including hydraulic jumps, using the Volume of Fluid (VoF) method (FLOW-3D® Version 2023R1 Users Manual (2023). FLOW-3D [Computer software]. Santa Fe, NM: Flow Science, Inc. https://www.flow3d.com). Numerical simulations are performed to compliment the results of the two methods (Experiments and Flow-3D), ascertain the accuracy of the results and fill the missing experimental data. The simulation model consisted of a rectangular flume, head tank, sluice and tail gates as shown in Fig. 3(a). In the present study, a Mass Momentum Source (MMS) is used as an inlet boundary condition, simulating a fluid source with a circular shaped pipe with diameter of 4 cm. This source allows a specified quantity of flow to enter the control volume of simulation,

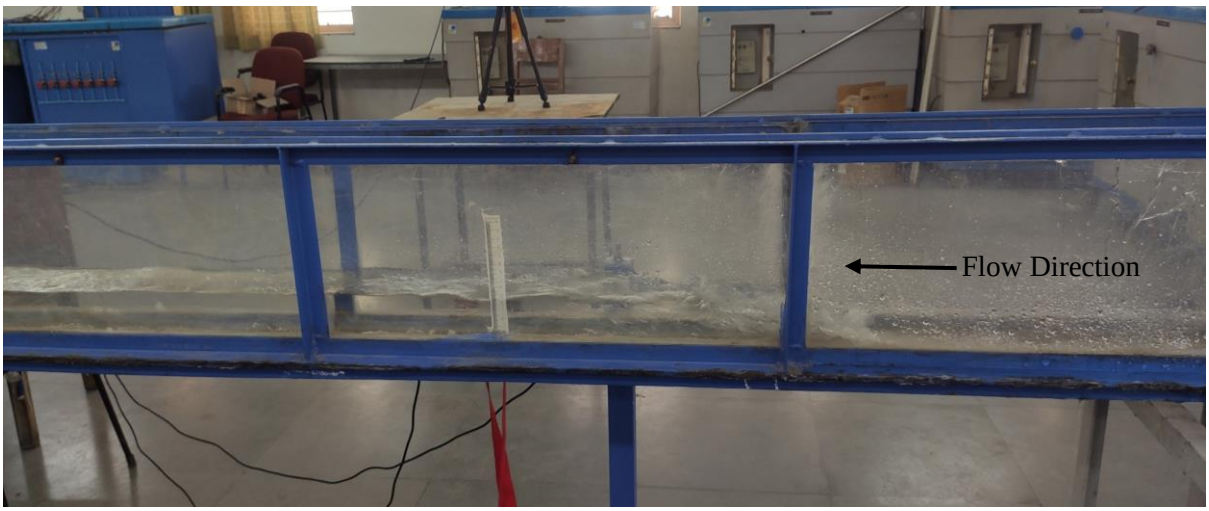

Fig. 2 Hydraulic jump occurring in the flume

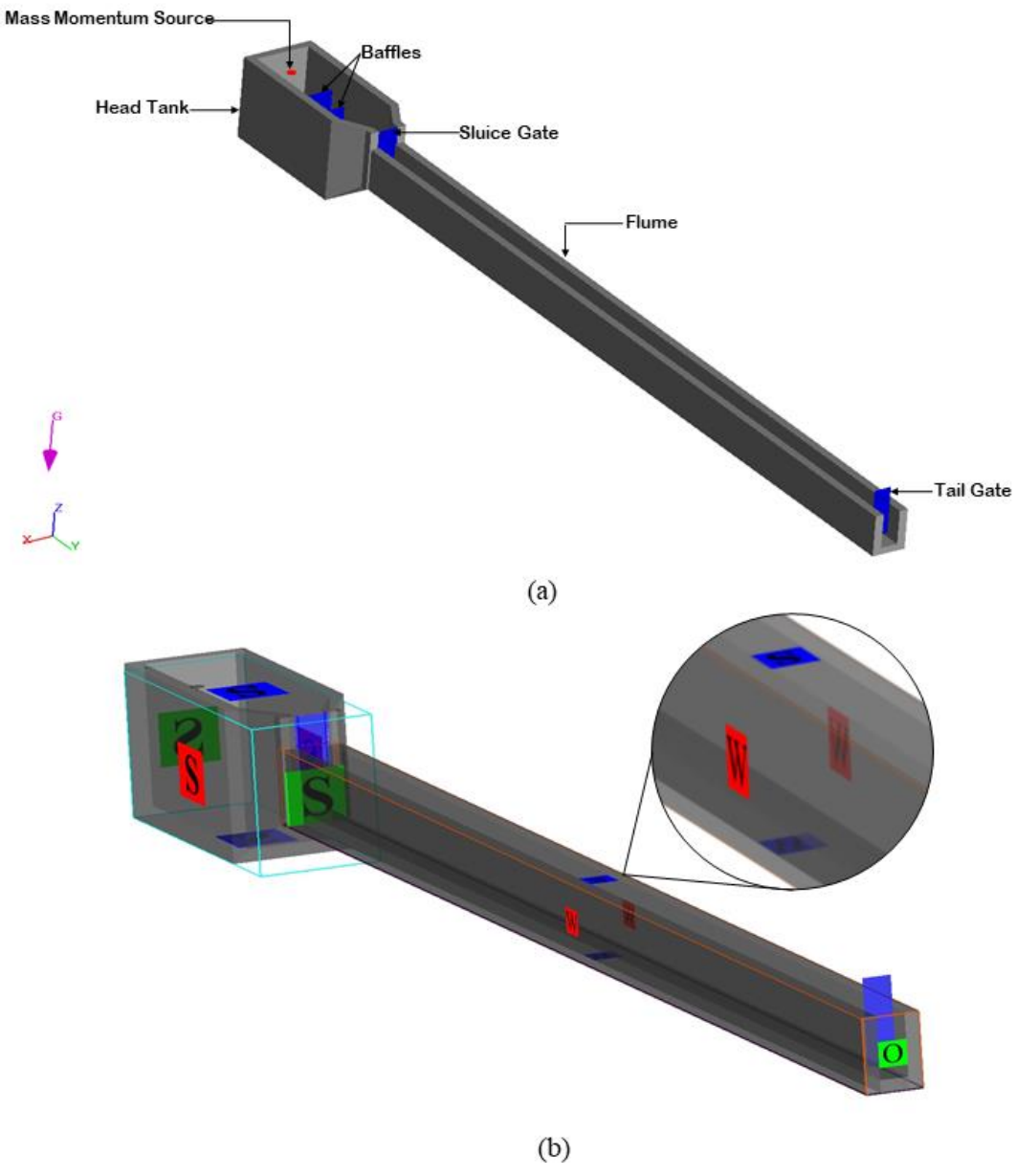

Fig. 3 (a) Geometry model used in Flow-3D for simulation, (b) Boundary conditions for each mesh plane of Flow-3D geometry

Table 2 Optimal mesh selection

Mesh Size (mm)	Mean Relative Error (%)	Simulation Time (h)
10	-13.55	2.1
7	-10.31	6.2
5	-6.28	21.6
3	-5.72	96.7

Table 3 Details of boundary conditions applied to mesh in Flow-3D

Geometry	Meshing Plane	Components	Boundary Condition
Flume	X-Min	Left wall	Wall
	X-Max	Right wall	Wall
	Y-Min	Inlet	Symmetry
	Y-Max	Outlet	Outflow
	Z-Min	Bed	Wall
	Z-Max	Free Surface	Symmetry
Head Tank	All Planes		Symmetry

replicating the exact conditions observed in experimental settings. The MMS is strategically located at the exact position where the actual pipe inlet is situated in the experimental flume, ensuring a realistic representation of the experimental setup providing same flow rate as that of experiments (Fig. 3 (a)).

Gravity and viscosity physics models were also added in the numerical simulations. The Renormalized group (RNG) κ-ε turbulence model was activated to simulate the turbulence in the flow. The meshing was provided to cover the geometry i.e., upstream head tank and flume with the computational domain. For identifying the optimal mesh size, numerical simulations were carried out for four mesh sizes as shown in Table 2. The mean relative error of flow depths measured across the entire flow profile of the hydraulic jump was calculated by comparing experimental data with numerical simulation results. The simulations were run until steady-state conditions were achieved, and the corresponding simulation time at which the flow became steady was recorded. It is observed that 5 mm and 3 mm meshing provided nearly same accuracy, however, 3 mm mesh require huge elapsed time of simulation. Therefore, 5 mm optimal mesh size was used for the simulations. Fractional area volume obstacle representation (FAVOR) method is used in Flow-3D to utilize the meshing over the geometry. The boundary conditions applied to the mesh of the channel included symmetry, outflow and wall as illustrated in Fig 3 (b) and Table 3.

Table 4 Relative error of numerical and experimental results

Graph	Mean Relative Error (%)	Max. Relative Error (%)
SGO = 0.011 m Fig. 5 (a)	3.89	7.48
SGO = 0.013 m Fig. 5 (b)	-6.28	-14.12
SGO = 0.015 m Fig. 5 (c)	2.76	6.72
SGO = 0.020 m Fig. 5 (d)	-5.84	-11.41
TGO = 0.023 m Fig. 6 (a)	5.03	8.81
SGO = 0.026 m Fig. 6 (b)	2.68	6.94

The symmetry boundary condition assumes that conditions outside the solution domain are identical to those on the internal boundary. This ensures that the flow passes smoothly through the two computational domains. It functions like a mirror that reflects all the flow distribution. Hence, if mesh consists of any geometry or free surface, it will treat as object or atmospheric condition accordingly. A wall boundary condition represents a solid, impermeable surface where the fluid cannot penetrate. An outflow boundary condition is applied at the domain's exit, allowing fluid to leave without reflecting back into the computational domain. (FLOW-3D® Version 2023R1 Users Manual, 2023)

Figure 4 displays the 3D output of the hydraulic jump formed between the sluice and tail gates after completion of the Flow-3D simulation. A comparison of flow profile of hydraulic jump between Flow-3D simulation and the experimental results is illustrated in Fig. 5 for different SGO. On the other hand, Fig. 6 demonstrates the correlation between experimental data and numerical simulations for change in TGO. Table 4 shows the relative error between numerical results and experimental data. The results show a satisfactory agreement between the numerical simulations and the experiments.

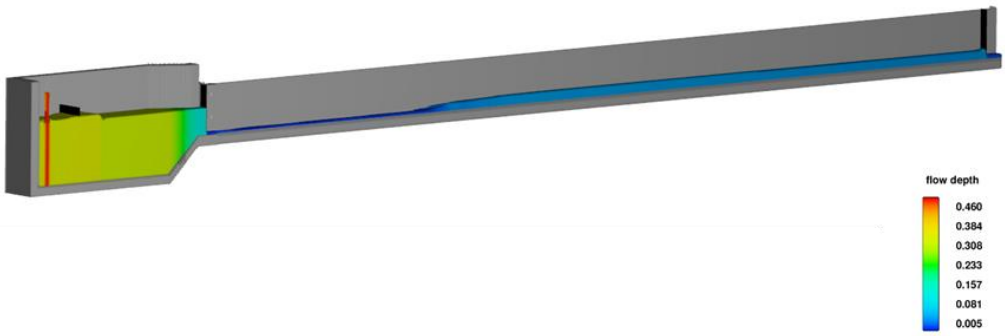

Fig. 4 Hydraulic jump 3D output in Flow-3D

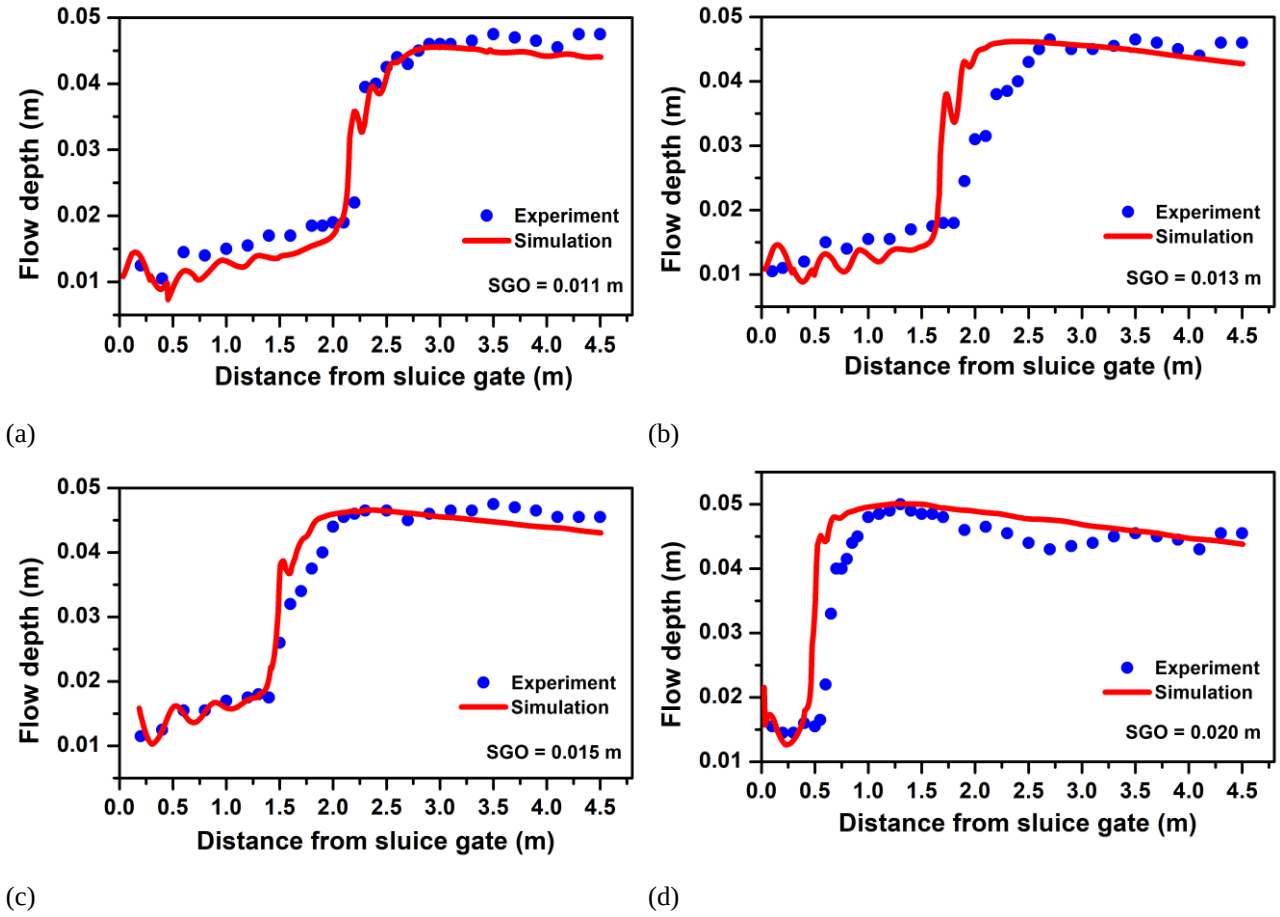

Fig. 5 Comparison of experimental data and numerical simulations for different sluice gate opening

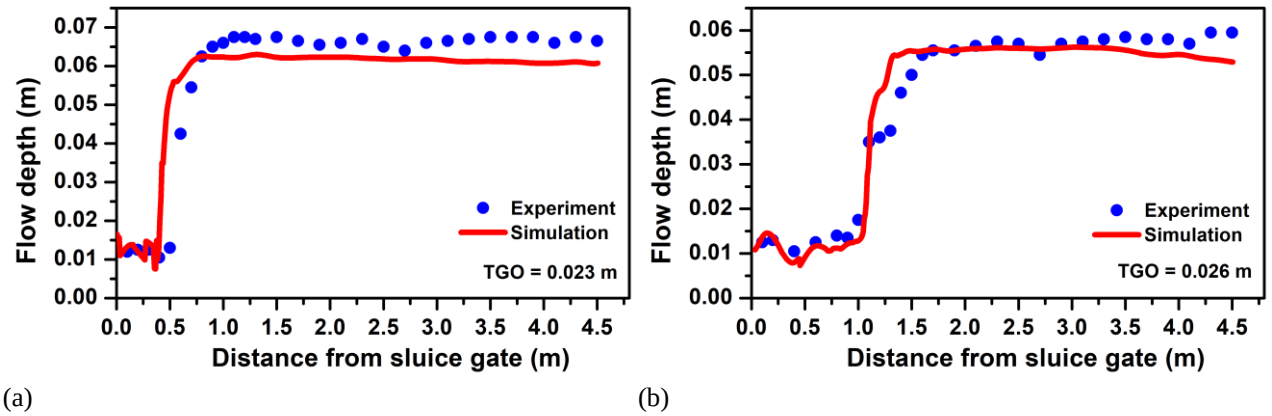

Fig. 6 Comparison of experimental data and numerical simulations for different tail gate opening

4. RESULT AND DISCUSSION

Hydraulic jump is studied for Froude numbers (Fr) ranging from 1.58 to 4.48 (Table 1), which according to Subramanya (2019) falls within the category of weak to oscillating hydraulic jump. The experiments were performed at the fixed discharge of 1.51×10^{-3} m^3/sec (Table 1). All measurements were taken once the hydraulic jump got stabilized. The flow entering the channel is regulated by sluice gate. Location and depth of the hydraulic jump are controlled by tail gate.

4.1 Effect of Sluice Gate Opening on Hydraulic Jump

Figure 7 and Table 5 illustrate the hydraulic jump for various SGO. It is observed that downstream depth (y_2) of the hydraulic jump does not change much with increasing SGO, but there is an evident change in upstream depth (y_1). Also, there is significant change in the location of hydraulic jump with change in SGO. For lower SGO, hydraulic jump forms farther from the sluice gate, with a higher y_1. As SGO increases, location of the jump shifts towards the sluice gate and y_1 decreases. This behaviour is observed due to the reduction in inlet velocity with increasing SGO, leading to an earlier formation of the hydraulic jump.

Table 5 Details of flow depth and location of hydraulic jump for varying SGO

SGO (m)	Upstream Flow Depth (m) (y_1)	Location of Hydraulic Jump (m)
0.011	0.019	2.1
0.013	0.018	1.8
0.015	0.0175	1.4
0.017	0.016	0.9
0.020	0.0155	0.55

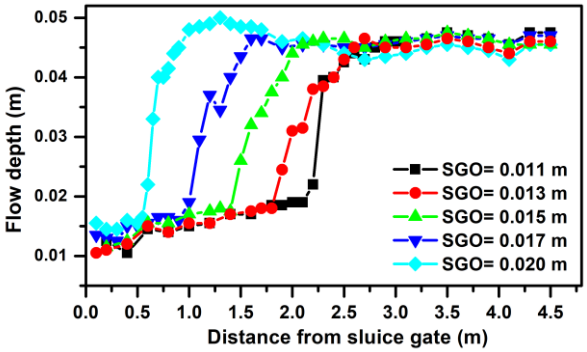

Fig. 7 Variation in hydraulic jump due to change in sluice gate opening

Table 6 Details of flow depth and location of hydraulic jump for varying TGO

TGO (m)	Upstream Flow Depth (m) (y_1)	Downstream Flow Depth (m) (y_2)	Location of Hydraulic Jump (m)
0.023	0.0105	0.0675	0.5
0.026	0.0135	0.0575	0.9
0.030	0.019	0.046	2.1

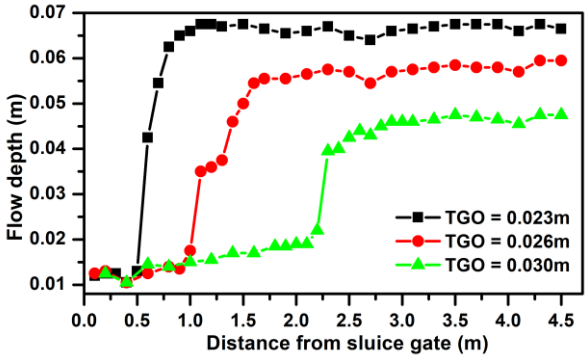

Fig. 8 Variation in hydraulic jump due to change in tail gate opening

4.2 Effect of Tail Gate Opening on Hydraulic Jump

Effect of TGO on hydraulic jump is presented in Fig. 8. It is observed from Fig. 8 and Table 6 that TGO has significant impact on upstream depth (y_1), downstream depth (y_2) and location of the hydraulic jump. The observations show that hydraulic jump shifts towards sluice gate with the reduction in TGO. Furthermore, the y_1 decreases, whereas the y_2 increases as the jump shifts towards the sluice gate due to decreasing TGO. This is due to the backwater effect in the channel. As TGO decreases, backwater increases, thereby shifting the location of hydraulic jump towards the sluice gate and rising the downstream depth (y_2).

4.3 Location of the Hydraulic Jump

Location of hydraulic jump is calculated theoretically using the classical equation below (Subramanya, 2019):

$$\Delta x = \frac{\Delta E}{S_0 - \bar{S_f}} \tag{1}$$

where, Δx is a step size of the theoretical location of hydraulic jump, ΔE is energy loss, S_0 is bed slope of channel and $\bar{S_f}$ is change in energy slope. The theoretical location of hydraulic jump (x) can be calculated by summation of Δx.

ΔE can be determined from the difference between specific energies (E). Similarly, $\bar{S_f}$ can be determined from the difference between energy slopes (S_f). E and S_f can be calculated with Eq. (2) and Eq. (3) respectively (Subramanya, 2019).

There are two basic assumptions involved in the analysis of Eq. (1) (Subramanya, 2019): 1. The pressure distribution at any cross section of the flow till the toe of the jump is assumed to be hydrostatic because streamlines have a small curvature. 2. The resistance to flow at any flow depth should be given by uniform flow equation, such as manning's formula, which in this case is given by energy slope (S_f).

$$E = y + \frac{V^2}{2g} \tag{2}$$

$$S_f = \frac{n^2 V^2}{R^2} \tag{3}$$

where, y is flow depth at corresponding Δx in the channel, V is flow velocity for corresponding y, n is manning's roughness coefficient, g is acceleration due to gravity and R is the hydraulic radius of the section at depth y.

The theoretical location of the hydraulic jump, calculated using Eq. (1), is compared with the experimental and simulation results in Fig. 9. A strong correlation is observed between the theoretical, experimental, and simulation values, demonstrating considerable accuracy in locating the jump.

The relationship between the variation in hydraulic jump location with SGO and TGO is studied. Figure 10 (a), shows the variation in jump location (x) for different SGO (d_s), and the corresponding equation to determine the jump location based on SGO is presented in Eq. (4). It is observed that, distance of hydraulic jump decreases with increasing SGO, as also demonstrated in Table 5. Similarly, Fig. 10 (b) illustrates the variation in jump location (x) for different TGO (d_t), and the equation to calculate the jump location based on TGO is provided in Eq. (5). It is observed that, distance of hydraulic jump increases with increasing TGO, which is consistent with the results in Table 6. Hence, Eq. (4) and Eq. (5) can be

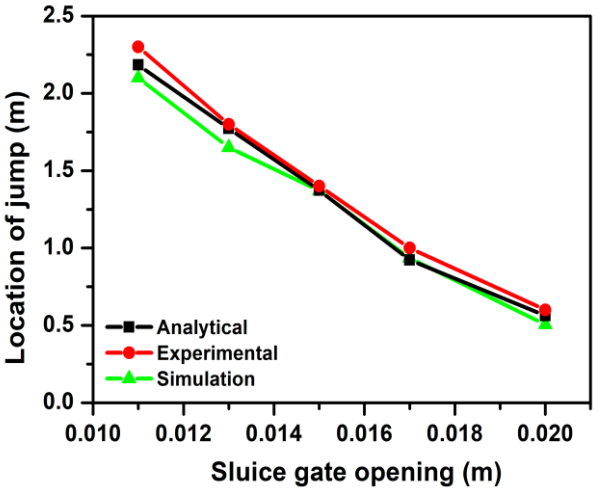

Fig. 9 A match between theoretical, experimental and simulation location of jump

used to control the hydraulic jump at a required location by adjusting SGO and TGO respectively. It is worth noting that, since only three experimental data points for TGO were available (Fig. 8 and Table 6), two numerical simulation data points had been added in Fig. 10(b) alongside the experimental data to facilitate a better analysis of relation between TGO and jump location.

$$x = 10^{-3.8597} \times {d_s}^{-2.1692} \quad (4)$$

$$x = 10^{8.9851} \times {d_t}^{5.6672} \quad (5)$$

where, x is location of hydraulic jump, d_s is sluice gate opening and d_t is tail gate opening. Eq. (4) and Eq. (5) were studied for the SGO range of 0.011 – 0.020 m and TGO range of 0.023 – 0.030 m respectively.

Figure 10 (c) presents the comparison of Eq. (4) (Fig. 10 (a)) with previous literature such as Yildiz et al. (2020) and Retsinis and Papanicolaou (2020). The results are observed to be closely matched with the existing data.

4.4 Energy Dissipation

Hydraulic jump results in significant amount of energy dissipation through transition of the flow (Singh & Roy, 2022). Sluice and tail gates influence the amount of energy dissipation due to their ability to control hydraulic jump as discussed in Sections 4.1-4.3. Energy dissipation in hydraulic jump can be expressed as Eq. (6) (Subramanya, 2019).

$$\Delta E = \frac{(y_2 - y_1)^3}{4 y_1 y_2} \quad (6)$$

where, ΔE is energy loss, y_1 and y_2 are upstream and downstream depths of hydraulic jump respectively. Table 7 shows the energy loss in hydraulic jump due to SGO and TGO. Table 7 consists of two numerical simulation data points for TGO (TGO = 0.025 m and 0.028 m), as discussed in Section 4.3, along with experimental data for the remaining TGO and SGO values.

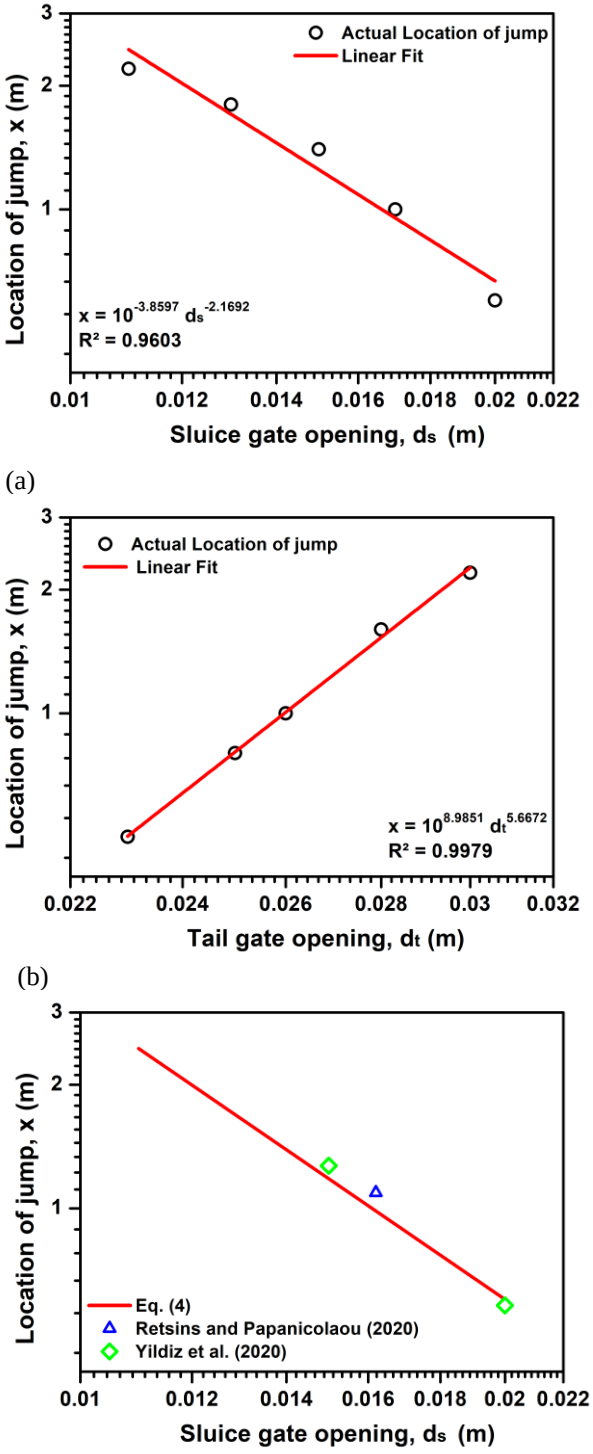

Fig. 10 (a) Relation of location of the jump and change in sluice gate opening; (b) Relation of location of the jump due to change in tail gate opening (c) Comparison of Eq. (4) with previous literature

Figure 11 compares the energy loss in associated with changes in SGO and TGO as depicted in Table 7. It is observed that TGO results in greater dissipation of energy than SGO. It is also concluded from Fig. 11 that energy dissipation increases gradually with increasing SGO. However, the energy dissipation increases drastically with decreasing TGO. The reason for this observation is explained in view of Fig. 7 & Fig. 8, which show that flow

Table 7 Energy loss in hydraulic jump for different SGO and TGO

SGO (m)	Energy Loss (m)	TGO (m)	Energy Loss (m)
0.011	0.0056	0.023	0.0653
0.013	0.0069	0.025	0.0393
0.015	0.0075	0.026	0.0274
0.017	0.0095	0.028	0.0154
0.020	0.0132	0.030	0.0056

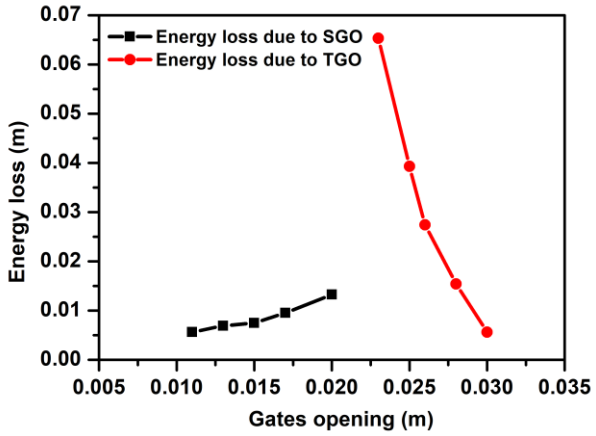

Fig. 11 Energy loss due to SGO and TGO

depth of hydraulic jump is considerably higher in the case of TGO compared to SGO due to the backwater effect. This results in more significant amount of energy dissipation in the presence of TGO.

Present study establishes that gates are highly effective for controlling the hydraulic jump. It has been concluded that reducing the TGO helps moving the hydraulic jump towards the sluice gate and increases the energy dissipation. This phenomenon forces the flow transition to occur close to the sluice gate within a short span of the channel length, thus preventing of damages caused by supercritical flow on the channel. Therefore, tail gate serves as a major energy dissipator by controlling depth and location of hydraulic jump.

5. CONCLUSION

Present study investigates the impact of sluice gate opening (SGO) and tail gate opening (TGO) on hydraulic jumps in a rectangular channel under steady state conditions. The study reveals that increasing SGO does not affect the downstream depth (y_2) of hydraulic jump significantly but upstream depth (y_1) decreases and its location shifts towards the sluice gate. While, decreasing TGO significantly affects both upstream (y_1) and downstream depth (y_2) and moves the jump towards the sluice gate. Additionally, location of the hydraulic jump is predicted theoretically and correlates well with experiments and numerical simulations. Eq. (4) and Eq. (5) can effectively determine the location of the hydraulic jump based on SGO and TGO respectively. Notably, TGO results in greater energy dissipation compared to SGO and can serve as a more efficient energy dissipator. The practical implications indicate that gates, particularly tail gates, are effective in controlling hydraulic jumps and managing energy dissipation, thereby preventing damage from supercritical flows in channels.

ACKNOWLEDGEMENTS

We are sincerely thankful to Flow Science, Inc., developer of the computational fluid dynamics (CFD) software, FLOW-3D® (https://www.flow3d.com) for making the FLOW-3D® HYDRO software available through the FLOW-3D Academic Program.

CONFLICT OF INTEREST

The authors declare that they have no conflict of interest.

AUTHORS CONTRIBUTION

Pratik D. Jiwane: Methodology, Investigation, Formal analysis, Software, Validation, Data Curation, Writing - Original Draft, Visualization. **Avinash D. Vasudeo:** Conceptualization, Methodology, Validation, Supervision, Writing - Review & Editing. **Arun Kumar Singh:** Conceptualization, Methodology, Validation, Supervision, Writing - Review & Editing.

REFERENCES

Babaali, H., Shamsai, A., & Vosoughifar, H. R. (2014). Computational modeling of the hydraulic jump in the stilling basin with convergence walls using CFD codes. *Arabian Journal for Science and Engineering*, *40*(2), 381–395. https://doi.org/10.1007/s13369-014-1466-z

Bayón, A., Valero, D., García-Bartual, R., Vallés-Morán, F. J., & López-Jiménez, P. A. (2016). Performance assessment of OpenFOAM and FLOW-3D in the numerical modeling of a low Reynolds number hydraulic jump. *Environmental Modelling and Software*, *80*, 322–335. https://doi.org/10.1016/j.envsoft.2016.02.018

Castro-Orgaz, O., & Hager, W. H. (2009). Classical hydraulic jump: Basic flow features. *Journal of Hydraulic Research*, 47(6), 744–754. https://doi.org/10.3826/jhr.2009.3610

Chanson, H. (2009). Current knowledge in hydraulic jumps and related phenomena. A survey of experimental results. *European Journal of Mechanics-B/Fluids*, *28*(2), pp.191-210. https://doi.org/10.1016/j.euromechflu.2008.06.004

Chern, M. J., & Syamsuri, S. (2013). Effect of corrugated bed on hydraulic jump characteristic using SPH method. *Journal of Hydraulic Engineering*, *139*(2), 221–232. https://doi.org/10.1061/(ASCE)HY.1943-7900.0000618

Chow, V. T. (1959). *Open channel hydraulics*. McGraw-Hill Book Co., Inc.

FLOW-3D® Version 2023R1 [Computer software]. (2023). Santa Fe, NM: Flow Science, Inc. https://www.flow3d.com

FLOW-3D® Version 2023R1 Users Manual. (2023). Santa Fe, NM: Flow Science, Inc. https://www.flow3d.com

Gharangik, A. M., & Chaudhry, M. H. (1991). Numerical simulation of hydraulic jump. *Journal of Hydraulic Engineering*, *117*(9), 1195–1211. https://doi.org/10.1061/(ASCE)0733-9429(1991)117:9(1195)

Gumus, V., Simsek, O., Soydan, N. G., Akoz, M. S., & Kirkgoz, M. S. (2016). Numerical modeling of submerged hydraulic jump from a sluice gate. *Journal of Irrigation and Drainage Engineering*, *142*(1), 04015037. https://doi.org/10.1061/(ASCE)IR.1943-4774.0000948

Gupta, U. P., & Ojha, C. S. P. (2013). Minimising interference of hydraulic jump with hydraulic gates. *ISH Journal of Hydraulic Engineering*, *19*(3), 179–185. https://doi.org/10.1080/09715010.2013.796689

Hager, W. H., & Bremen, R. (1989). Classical hydraulic jump: sequent depths. *Journal of Hydraulic Research*, 27(5), 565–585. https://doi.org/10.1080/00221688909499111

Hafnaoui, M. A., & Debabeche, M. (2021). Numerical modeling of the hydraulic jump location using 2D Iber software. *Modeling Earth Systems and Environment*, *7*(3), 1939–1946. https://doi.org/10.1007/s40808-020-00942-3

Kim, Y., Choi, G., Park, H., & Byeon, S. (2015). Hydraulic jump and energy dissipation with sluice gate. *Water MDPI*, *7*(9), 5115–5133. https://doi.org/10.3390/w7095115

Mirzaei, H., & Tootoonchi, H. (2020). Experimental and numerical modeling of the simultaneous effect of sluice gate and bump on hydraulic jump. *Modeling Earth Systems and Environment*, *6*(4), 1991–2002. https://doi.org/10.1007/s40808-020-00835-5

Mnassri, S., & Triki, A. (2022). Numerical investigation towards the improvement of hydraulic-jump prediction in rectangular open-channels. *ISH Journal of Hydraulic Engineering*, *28*(2), 135–142. https://doi.org/10.1080/09715010.2020.1836684

Nandi, B., Das, S., & Mazumdar, A. (2020). *Experimental analysis and numerical simulation of hydraulic jump*. IOP Conference Series: Earth and Environmental Science, 505, 012024. https://doi.org/10.1088/1755-1315/505/1/012024

Ohtsu, I., & Yasuda, Y. (1994). Characteristics of supercritical flow below sluice gate. *Journal of Hydraulic Engineering*, *120*(3), 332–346. https://doi.org/10.1061/(ASCE)0733-9429(1994)120:3(332)

Paik, J., & Kim, B. (2023). Large eddy simulation of a steady hydraulic jump at Fr = 7.3. *Journal of Korea Water Resources Association*, *56*(1), 1049–1058. https://doi.org/10.3741/JKWRA.2023.56.S-1.1049

Rajaratnam, N. (1977). Free flow immediately below sluice gates. *Journal of the Hydraulics Division*, *103*(4), 345–351. https://doi.org/10.1061/JYCEAJ.0004729

Retsinis, E., & Papanicolaou, P. (2020). Numerical and experimental study of classical hydraulic jump. *Water*, *12*(6), 1766. https://doi.org/10.3390/w12061766

Roushangar, K., Ghasempour, R., & Valizadeh, R. (2018). Effect of channel boundary conditions in predicting hydraulic jump characteristics using an ANFIS-based approach. *Journal of Applied Fluid Mechanics*, 11(3), 555-565. https://doi.org/10.29252/jafm.11.03.27933

Singh, U. K., & Roy, P. (2022). Energy dissipation in hydraulic jumps using triple screen layers. *Applied Water Science*, *13*(1). https://doi.org/10.1007/s13201-022-01824-y

Singha, S. B., Bhattacharjee, J. K., & Ray, A. K. (2005). Hydraulic jump in one-dimensional flow. *The European Physical Journal B*, *48*(3), 417–426. https://doi.org/10.1140/epjb/e2005-00404-0

Subramanya, K. (2019). *Flow in open channels*. Tata McGraw-Hill Education.

Wang, H., & Chanson, H. (2015). Experimental study of turbulent fluctuations in hydraulic jumps. *Journal of Hydraulic Engineering*, *141*(7), 04015010. http://doi.org/10.1061/(ASCE)HY.1943-7900.0001010

Yıldız, A., Martı, A.İ., Yarar, A., & Yılmaz, V. (2020). Determination of position of hydraulic jump in a flume by using CFD and comparison with experiential results. *Romanian Journal of Ecology and Environmental Chemistry*. https://doi.org/10.21698/rjeec.2020.211